OPTIMIZED DESIGN OF COMPLEX MICROCHANNEL HEAT SINK STRUCTURE WITH TRIANGULAR CAVITY M-TYPE PINS

Aiyun Wang and Zhongliang Pan

School of Electronics Science and Engineering, South China Normal University,

Foshan, 528225, China.

* Corresponding author;Email: panzhongliang@m.scnu.edu.cn

In order to further improve the heat dissipation performance of microchannels, a new triangular cavity M-type pin complex microchannel heat sink structure design is proposed. Firstly, we take the distance between the cavity center and the pin center of the microchannel heat sink, the pin width and the pin angle as design variables. The enhanced heat transfer factor of the microchannel heat sink is used as the objective function. Secondly, in this paper, a quadratic regression model between the independent variables and the enhanced heat transfer factor of the microchannel radiator is established by the response surface method, and the design variables are optimized by combining the genetic algorithm to maximize the enhanced heat transfer factor. The results show that the optimized microchannel heat sink can achieve the optimal distribution of pressure field and temperature field, and the enhanced heat transfer factor can achieve the optimal value, which can significantly improve the heat dissipation performance of the microchannel and provide an important reference for the subsequent microchannel optimization design.

Key words: microchannel heat sink, pins, enhanced heat transfer factor, response surface, genetic algorithm

1. Introduction

With the rapid development of microelectronic devices in the direction of integration, miniaturization and high stability, their heat generation has exceeded 10^6 W/m². The microchannel fluid heat transfer technology has demonstrated excellent thermal management capabilities due to its small temperature difference in heat transfer, high heat transfer efficiency, making it an ideal solution for addressing the high heat flux density heat dissipation problem of microelectronic devices [1]. Microchannel heat dissipation technology was first proposed by Tuckerman and Pease of Stanford University in 1981 [2]. As pioneers in the field of microchannel heat sinks, they conducted the first experimental research on microchannel heat transfer, laying the groundwork for experimental methods

and theoretical foundations that would support the subsequent innovation and optimization of microchannel heat sinks. Since then, microchannel heat dissipation technology has attracted numerous researchers both domestically and internationally. These researchers have analyzed the heat transfer performance of microchannels using experiments and numerical simulations. These researchers have analyzed the heat transfer performance of microchannels using experiments and numerical simulations, this mainly includes the following four aspects:

(1) Researchers have determined the optimal geometric shape for heat dissipation by studying the impact of microchannel fin geometry on heat transfer[3]. Acharya et al.[4] investigated the effects of square and elliptical fins on heat dissipation and friction under different arrangements. Wen et al.[5] explored the thermal performance of microchannel heat sinks with differently shaped fins combined with secondary channels. Wu et al.[6] studied the fluid distribution and heat transfer in microchannel heat sinks with rectangular flow. Hu et al.[7] examined the characteristics of open microchannel heat sinks with trapezoidal cover plates.

(2) Researchers have determined the optimal geometric structure for heat dissipation by studying the impact of microchannel heat sink structures on heat transfer. Hajialibabaei et al.[8] investigated the effect of microchannel channel heat sink heights on thermal performance. Shi et al.[9] examined the influence of irregular polygonal topologies in multi-branch microneedle fin heat sinks on thermal performance. Kamsuwan et al.[10] studied the heat dissipation performance of inclined double-layer plate microchannel heat exchangers. Fathi et al.[11] explored the application of forked diverging microchannel heat sinks in microelectronics cooling.

(3) Researchers have determined the optimal interface configuration for heat dissipation by studying the impact of microchannel heat sink interface configurations on heat transfer. Kang et al.[12] investigated the effects of different interface configurations on the heat transfer performance of manifold microchannel heat sinks. Amit et al.[13] studied the heat transfer characteristics when fluids pass through microchannels with hot spots.

(4) Researchers have determined the fluid materials with optimal heat dissipation effects by studying the impact of fluid materials on heat transfer in microchannel heat sinks. Liu et al.[14] investigated the flow and heat transfer characteristics of water-based microcapsule phase change material suspensions in microchannels with different fin structures. Zhou et al.[15-16] investigated the application of nanofluid structures with varying concentrations in enhancing the heat transfer mechanism for heat dissipation in high heat flux density electronic devices.

With the widespread application of various optimization algorithms, researchers have used these algorithms to optimize the geometric structures of microchannel coolers[17]. A. Rabiee et al.[18-19] optimized the geometric parameters of different microchannel coolers using the NSGA-II algorithm for different objective functions and predicted the optimal geometric structures. Zhang et al.[20] used genetic algorithms to verify that most needle-ribbed MMC designs can simultaneously reduce both the pressure drop and thermal resistance of chips. Cheng et al.[21] employed BP neural networks and the

NSGA-II algorithm to perform multi-objective optimization of thermal resistance and pressure drop for microchannels with different groove widths and channel depths, thereby determining the optimal groove width. Wang et al.[22] used the NSGA-II algorithm combined with the TOPSIS method based on information entropy weighting to obtain the optimal heat transfer scheme design for symmetric hierarchical microchannel coolers.

To explore a more advanced microchannel heat sink structure, this paper proposes a novel triangular cavity M-type microchannel heat sink design. The design variables include the distance between the cavity center and the pin center of the microchannel heat sink, the pin width and the pin angle. The objective function is the enhanced heat transfer factor of the microchannel. This paper then applies response surface methodology combined with genetic algorithms to optimize the enhanced heat transfer factor of the microchannel heat sink, thereby achieving a geometric structure that ensures optimal microchannel heat sink performance. This design provides a novel and effective approach for optimizing microchannel heat sinks.

2. Numerical simulation of microchannel heat sink

2.1. Microchannel heat sink model

This paper references the microchannel heat sink model with trapezoidal cavity and elliptical pins proposed by Alfellag et al.[23], and designs a three-dimensional model of a triangular cavity M-type pin microchannel heat sink using COMSOL Multiphysics software. The design parameters of the microchannels are shown in Tab1. The design drawings of the microchannels are shown in Fig1.

Table 1. Geometric parameters of triangular cavity M-type pin microchannel

Parameters	Value	Unit	Parameters	Value	Unit	Parameters	Value	Unit
L	0	mm	***l***	10	mm	***a***	0.3	mm
W	0.3	mm	***w***	0.1	mm	***b***	0.08	mm
H	0.35	mm	***h***	0.2	mm	c_1	0.2	mm
s	3100	μm^2	***d***	4	mm	c_2	0.2	mm
A	0-10	μm	***B***	8-12	μm	***C***	60-120	°
D	3	mm						

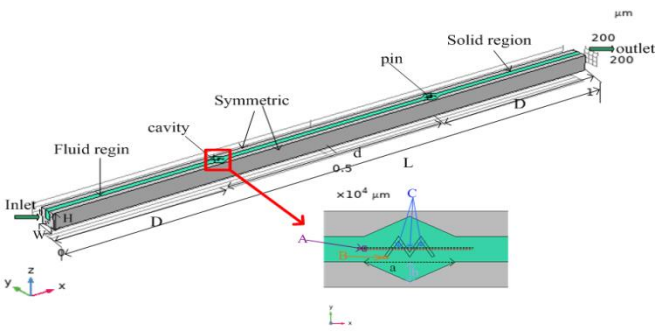

Figure 1. Schematic diagram of the geometry of triangular cavity M-type pin microchannel

The length *L*, width *W*, and height *H* of the triangular cavity M-type pin micro-channel heat sink calculation domain are 10 mm, 0.3 mm, and 0.35 mm respectively. The length *l*, width *w*, and height *h* of a single micro-channel heat sink are 10 mm, 0.1 mm, and 0.2 mm respectively. There are two cavities and two M-type pins along the flowing axis, the area of the cavities and the volume of the pins are consistent with the model proposed by Alfellag. The bottom length *a*, top length *b*, and height c_1 of the cavity are 0.3 mm, 0.08 mm, and 0.2 mm respectively. The height c_2 of the M-type pin is 0.2 mm, and the top area *s* is 3100 μm². The range of distance *A* from the cavity center to the pin center, the range of pin width *B*, and the range of pin angle *C* are 0-10 μm, 8-12 μm, and 60-120 degrees respectively. The distance *D* from the micro-channel inlet and outlet to the cavity center is 3 mm, and the distance *d* between the two cavities is 4 mm.

2.2. Control equations and boundary conditions for microchannel heat sink

The microchannel heat sink in this paper uses aluminum as the base material of the microchannel. The base bottom supplies a heat flux of 1000 kW/m², and the inlet temperature is set to 300 K. The water is used as the fluid coolant of the microchannel in this paper, and the inlet speed is set to 10.27 m/s.

In order to analyze the flow and heat transfer characteristics of microchannels, the following assumptions are proposed:

(1) The fluid is a steady, incompressible Newtonian fluid, and the flow state is laminar.

(2) The properties of both fluid and solid are constant.

(3) Ignore other forms of physical forces such as thermal radiation and gravity.

Based on the above assumptions, the control equations include the continuity equation, momentum equation and energy equation as follows:

$$\nabla \cdot \vec{V} = 0 \tag{1}$$

$$\rho\left(\vec{V} \cdot \nabla\vec{V}\right) = -\nabla P + \nabla\left(\mu_f \cdot \nabla\vec{V}\right) \tag{2}$$

$$\rho C_p \vec{V} \cdot \nabla T_f = \nabla(\lambda_f \cdot \nabla T_f) \tag{3}$$

For solid regions, the energy equation is as follows:

$$\nabla(\lambda_z \cdot \nabla T_z) = 0 \tag{4}$$

In the above equation: $\vec{V}$ is the velocity of the fluid, *P* is the pressure in the fluid region, T_f is the temperature of the fluid, T_z is the temperature of the solid, while $\mu_f, \rho, C_p, \lambda_f$ and λ_z represent the dynamic viscosity coefficient, density, specific heat capacity, thermal conductivity of the fluid, and thermal conductivity of the solid, respectively. Water serves as the coolant for the microchannel, with a density of 1000 kg/m³, a thermal conductivity of 0.6 $W \cdot m^{-1} \cdot K^{-1}$, and a viscosity coefficient of 854.5 μPa·s.

2.3. Data acquisition formula of microchannel heat sink

The calculation relationship of Reynolds number in microchannel is as follows:

$$Re = \frac{\rho u D_h}{\mu_f} \tag{5}$$

In the above formula, u is the average velocity of the fluid, unit m/s; D_h is the hydraulic diameter of the microchannel.

The hydraulic diameter is used to describe the characteristics of fluid flow in non-circular pipes or channels. It is defined as four times the cross-sectional area divided by the wetting perimeter, and the calculation formula is as follows:

$$D_h = \frac{2hw}{h+w} \tag{6}$$

The inlet and outlet pressure drop (ΔP) of the microchannel reflects the energy consumption, which can be used to calculate the average friction coefficient. The calculation formula of inlet and outlet pressure drop and average friction coefficient is as follows:

$$\Delta P = P_{in} - P_{out} \tag{7}$$

$$f = \frac{2D_h \Delta P}{L\rho u^2} \tag{8}$$

In the above formula, P_{in} is the average inlet pressure of the microchannel, P_{out} is the average outlet pressure of the microchannel, and f is the average friction coefficient of the microchannel.

The average heat transfer coefficient (h_{av}) of the microchannel reflects the heat transfer ability between the fluid and the wall surface of the microchannel. It is an important parameter to describe the heat transfer performance of the microchannel. The higher the heat transfer coefficient, the more efficient the heat transfer is. The calculation formula is as follows:

$$h_{av} = \frac{q_w A_1}{A_2(T_1 - T_2)} \tag{9}$$

In the above formula, q_w is the heat flux density of the microchannel, unit is W/(m^2·K); A_1 is the heat of the heating surface of the microchannel; A_2 is the contact area between the fluid and the solid; T_1 is the average temperature of the contact surface between the fluid and the solid; T_2 is the average temperature of the fluid.

The Nusselt number (Nu) of the microchannel is an important index to reflect the convective heat transfer capacity in the microchannel. The larger average heat transfer coefficient (h_{av}), the larger the Nusselt number. The calculation formula is as follows:

$$Nu = \frac{h_{av} D_h}{\lambda_f} \tag{10}$$

The enhanced heat transfer factor is a dimensionless parameter proposed by Webb et al.[24], which can measure the comprehensive heat transfer performance of microchannels, and is also the objective function in this paper. The calculation formula is as follows:

$$PEC = \frac{Nu/Nu_0}{(f/f_0)^{1/3}} \tag{11}$$

In the above formula, where Nu_0 and f_0 stand for the Nusselt number and the average friction coefficient of the smooth straight microchannel respectively, while Nu and f stand for those of the cavity pin microchannel respectively.

3. Optimization of microchannel heat sink

3.1. Experimental design and simulation calculation based on Box-Behnken

The Response Surface Methodology (RSM), jointly proposed by Box and Wilson, is a technique used in industrial design and other fields to optimize experimental design and data analysis. The Box-Behnken Design (BBD) method, as one type of Response Surface Optimization Analysis, arranges experimental points in the middle-level regions of the experimental space to avoid extreme levels of factors, thereby reducing the number of experiments and minimizing the instability risk associated with extreme conditions. It fits a multivariate quadratic regression equation to determine the functional relationship between each factor and the response value. The Design Expert software was used to design 17 sets of three-factor three-level test groups with *PEC* as the response and *A*, the distance between the center of the microchannel heat sink cavity and the center of the pin, *B*, the width of the pin, and *C*, the angle of the pin, as the independent variables (the range of *A*, *B* and *C* was 0-10 μm, 8-12 μm and 60-120° respectively). The enhanced heat transfer factor value of each test group is calculated by numerical simulation using COMSOL Multiphysics software. The specific test data and *PEC* value of the microchannel heat sink are shown in Tab2.

Table 2. Data and PEC value of microchannel heat sink test design group

Number	*A*（μm）	*B*（μm）	*C*（°）	*PEC*	Number	*A*（μm）	*B*（μm）	*C*（°）	*PEC*
1	0	12	60	1.823	**10**	5	12	60	1.82
2	10	8	90	1.729	**11**	10	12	60	1.817
3	0	12	90	1.826	**12**	5	12	120	1.796
4	10	12	90	1.824	**13**	5	8	120	1.724
5	0	10	60	1.826	**14**	0	10	90	1.827
6	10	10	60	1.82	**15**	5	10	90	1.807
7	0	10	120	1.802	**16**	10	10	90	1.807
8	10	10	120	1.804	**17**	0	8	60	1.755
9	5	8	60	1.738					

3.2. Fitting analysis of the enhanced heat transfer factor response surface model

In this paper, the polynomial function of the enhanced heat transfer factor fitted by the BBD method is as follows:

$$PEC = 0.715009 - 0.009905A + 0.199567B + 0.000853C + 0.000434AB + 0.000016AC - 0.00000640605BC + 0.000312A^2 - 0.009075B^2 - 0.00000635139C^2 \quad (12)$$

The results of variance analysis of the enhanced heat transfer factor regression model are shown in Tab3. The P-value measures the deviation between the model's predicted values and the actual observations, for the influencing factors in the model, P value less than 0.05 indicates that it is significant. The regression model for the enhanced heat transfer factor has an F-value of 75.17 and a P-value below 0.01, indicating high significance. The P-values for factors A, B, and C are all below 0.05, meaning they all significantly affect the enhanced heat transfer factor.

Table 3. Analysis of variance table for the response surface model of the enhanced heat transfer factors

Source	Sum of Squares	Mean Square	F-value	P-value
Model	0.0206	0.0023	75.17	<0.0001
A	0.0002	0.0002	7.62	0.0279
B	0.0125	0.0125	410.82	<0.0001
C	0.0006	0.0006	20.07	0.0029

The analysis results of the regression equation of heat transfer factor in this paper are shown in Tab4. The correlation coefficients (R^2, Adj R^2, and Pre R^2) are all close to 1, indicating good fitting, performance, and predictive power of the enhanced heat transfer factor model. The difference between Adj R^2 and Pre R^2 is less than 0.2, Adeq Precision is greater than 4, and the coefficient of variation (C.V.%) of the regression equation is 0.307, indicating that the enhanced heat transfer factor data shows minimal dispersion and that the model fits very successfully.

Table 4. Regression equation analysis of the enhanced heat transfer factor

Project	Std.Dev.	Mean	C.V.%	R^2	Adjusted R^2	Predicted R^2	Adeq Precision
Value	0.0055	1.80	0.307	0.9898	0.9766	0.9264	25.257

The residual analysis diagram of the heat transfer factor model in this paper is shown in Fig2. The residuals of the enhanced heat transfer factors show a normal distribution and are on a line, and the

predicted residual values of the enhanced heat transfer factors are distributed between -4~4, which are randomly distributed and scattered, and the predicted and actual values of the enhanced heat transfer factors basically fall on the fitting curve, indicating that the fitting degree of the enhanced heat transfer factor model is better.

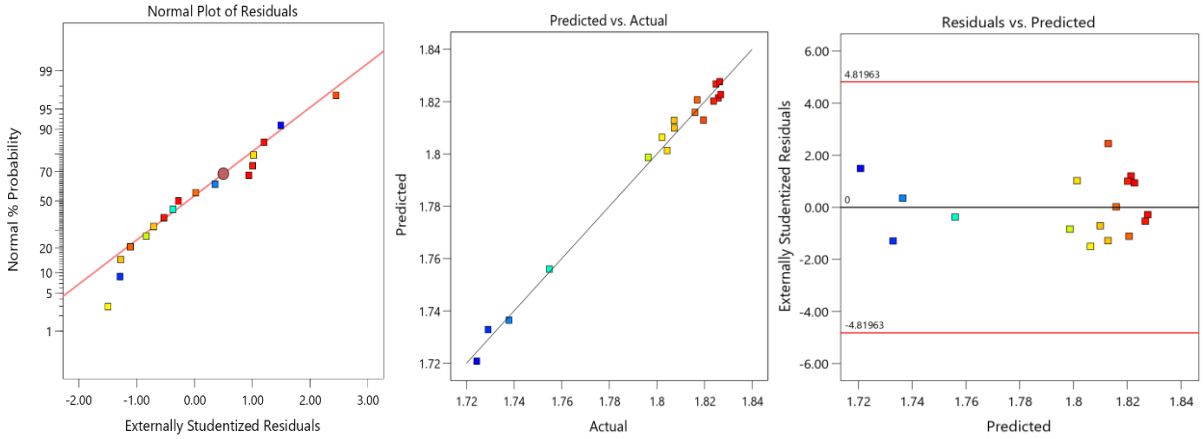

Figure 2. Residual analysis of the enhanced heat transfer factor model (a) Normal plot of residuals (b) Predicted and actual values (c) Residuals and predicted values

3.3. Genetic algorithm optimization of microchannel heat sink

In order to obtain a high-performance heat transfer microchannel design, this paper takes the enhanced heat transfer factor that can measure the comprehensive heat transfer performance of the microchannel as the objective function, combined with the polynomial function of the enhanced heat transfer factor fitted by the BBD method, and optimizes the optimal microchannel design of the M-shaped pin of the triangle cavity through genetic algorithm. The mathematical model of the optimized problem can be described as:

$$\begin{aligned} max\ \ f(A,B,C) \ &= \ max\ \{PEC(A,B,C)\} \\ s.t. \quad & 0 < A < 10 \quad (unit: \mu m) \\ & 8 < B < 12 \quad (unit: \mu m) \\ & 60 < C < 120 \quad (unit: \ ^\circ) \end{aligned} \tag{13}$$

In this paper, the population size is set as 50, the maximum number of iterations is 100, the crossover rate is 0.8, the variation rate is 0.01, and the fitness function is the objective function microchannel heat sink enhanced heat transfer factor *PEC*. The genetic algorithm first randomly generates the initial population by calling the random number function, and uses the computational function to calculate the fitness (*PEC* value) of each individual. Then, the selection operation is realized by the roulette selection method, the crossover operation is realized by generating new offspring by single-point crossing, and the mutation operation is realized by randomly changing the genes of some individuals to increase the diversity of the population. In each generation, genetic algorithms

sequentially perform fitness calculations, selection, crossovers, and mutation operations to generate new populations. Finally, after 100 iterative calculations, the enhanced heat transfer factor converges to 1.836. The fitness curve of global optimization by genetic algorithm is shown in Fig3.

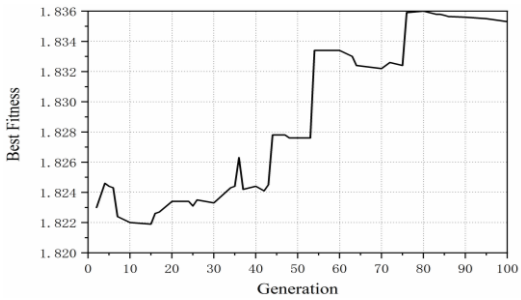

Figure 3. Fitness curve of global optimization by genetic algorithm

4. Results and analysis of microchannel heat sink

4.1. Response surface result analysis

The 3D response surface of PEC, which is obtained by BBD method for the triangular cavity M-type pin microchannel heat sink, is shown in Fig4. It intuitively illustrates the relationship between the distance *A* from the center of the microchannel cavity to the center of the pin, the pin width *B*, the pin angle *C*, and the enhanced heat transfer factor *PEC*, clearly showing the trend of how these factors affect the response value.

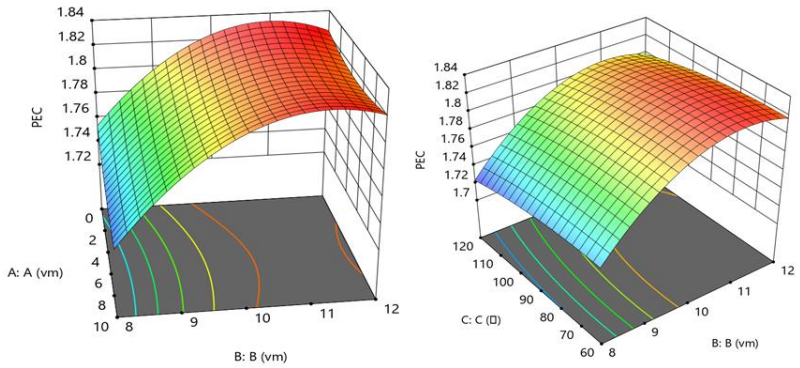

Figure 4. 3D response surface of the enhanced heat transfer factor

The velocity and pressure diagrams of the X-Y section of the microchannel heat sink under different *A*, *B* and *C* obtained by numerical simulation through COMSOL Multiphysics software are shown in Fig5:

The enhanced heat transfer factor of the microchannel heat sink gradually decreases with the increase of the distance *A* between the cavity center and the pin center as shown in Fig4. This is because a smaller distance between the cavity center and the pin center results in stronger turbulence generated by the microchannel fluid at the M-pin, which promotes the mixing of cold and hot fluids and improves

the heat transfer efficiency of the microchannel. As shown in Fig5(a), when A = 0 μm, the turbulence generated at the M-pin is stronger.

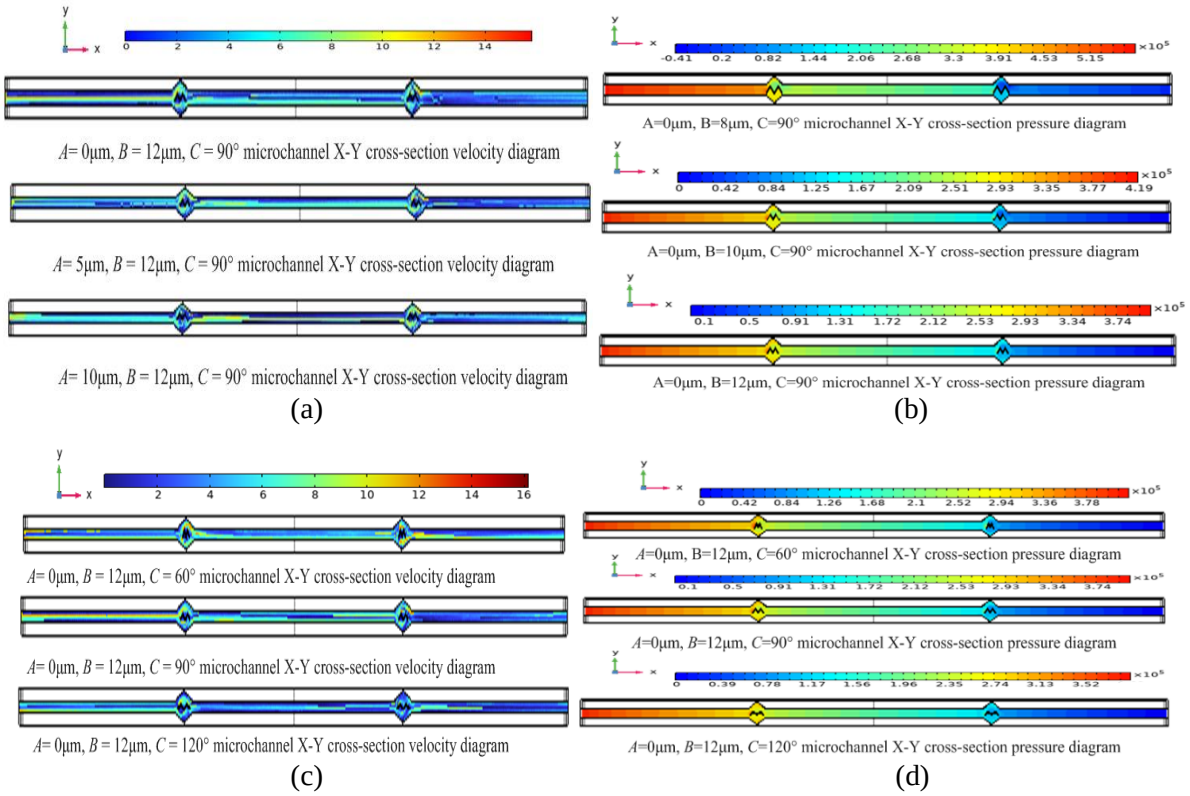

Figure 5. X - Y cross - sectional pressure and velocity distributions of the microchannel under varying A, B, C (a) Velocity with different A (B = 12 μm, C = 90°) (b) Pressure with different B (A = 0 μm, C = 90°) (c) Velocity with different C (A = 0 μm, B = 12 μm) (d) Pressure with different C (A = 0 μm, B = 12 μm)

The enhanced heat transfer factor of the microchannel heat sink increases and then decreases with the increase of pin width B as shown in Fig4. This is because as the pin width gradually decreases, the contact area between the M-pin and the water flow increases, the flow intensity increases, and the heat transfer is enhanced. However, at the same time, the reduction in pin width will enhance its resistance to water flow, leading to a rapid rise in the overall pressure drop of the microchannel. A larger pressure drop can lead to the deterioration of the enhanced heat transfer performance of the microchannel. As shown in Fig5(b), the overall pressure drop of the microchannel is greatest when B = 8 μm. The enhanced heat transfer factor of the microchannel heat sink increases and then decreases with the increase of pin angle C as shown in Fig4. This is because when the M-pin angle increases, the turbulence at the pin weakens, reducing the mixing of cold and hot fluids and thus weakening the heat transfer performance of the microchannel. However, an increased M-pin angle also reduces the overall pressure drop of the microchannel. As shown in Fig5(c), the turbulence generated by the M-pin is stronger at C = 60°, and as shown in Fig5(d) the overall pressure drop of the microchannel is greatest when C = 60°.

4.2. Analysis of optimization results of microchannel heat sink

The optimal microchannel design parameters *PEC* predicted by the Numerical function of the response surface method and the corresponding numerical simulation values are shown in Tab5. The optimal microchannel design parameters *PEC* predicted by the response surface method combined with genetic algorithm and the corresponding numerical simulation values are shown in Tab6. The data in the table show that the *PEC* prediction value of response surface method is 1.829, and the numerical simulation value is 1.832, with a relative error of 0.16%.The *PEC* prediction value of the response surface method combined with genetic algorithm is 1.836, and the numerical simulation value is 1.84, with a relative error of 0.21%.The errors of the two optimization methods are small, but in comparison, the structural parameters found by the response surface method combined with genetic algorithm have a larger value of the enhanced heat transfer factor *PEC*.

Table 5. *PEC* prediction value based on response surface method and corresponding numerical simulation *PEC* value

Parameters	*A*(μm)	*B*(μm)	*C*(°)	Predicted Value PEC	Numerical Simulation Value PEC	Relative Error（%）
Value	1.52	10.59	70.61	1.829	1.832	0.16

Table 6. *PEC* prediction value and corresponding numerical simulation *PEC v*alue based on response surface method combined with genetic algorithm

Parameters	*A*(μm)	*B*(μm)	*C*(°)	Predicted Value PEC	Numerical Simulation Value PEC	Relative Error（%）
Value	0.37	10.96	68.39	1.836	1.84	0.21

In this paper, the structural parameters of A=10 μm, B=10 μm, and C=60° were selected from 17 groups of unoptimized microchannel structures for numerical simulation, and compared with the numerical simulation values of A=0.37 μm, B=10.96 μm, and C=68.39° optimized by the response surface method combined with genetic algorithm, as shown in Tab7.

Table 7. Comparison of numerical simulation values before and after optimization

Project	*A*(μm)	*B*(μm)	*C*(°)	Import and export pressure drop (Pa)	*Nu*	*f*	PEC
Before Optimization	10	10	60	421157	34.076	0.106	1.82
After Optimization	0.37	10.96	68.39	417961	34.363	0.105	1.84

As shown in Tab7, after optimization, the average pressure drop across the microchannel inlet and outlet decreased by 3196 Pa, the average Nusselt number increased by 0.84%, and the overall heat transfer performance of the microchannel improved by 0.02. This achieved the goal of enhancing the heat transfer performance of the microchannel while reducing its overall pressure drop. It is evident that through the use of response surface method combined with genetic algorithms for global optimization,

the overall pressure drop of the microchannel was successfully reduced, and the heat transfer performance was improved.

The pressure diagrams before and after the optimization of the microchannel are shown in Fig6. Compared to before optimization, the overall pressure drop after optimization is reduced by 2722 Pa. The friction coefficient reflects the magnitude of flow resistance in the microchannel, specifically, the greater the flow resistance, the higher the friction coefficient; conversely, the lower the flow resistance, the smaller the friction coefficient. As can be seen from Tab7, the friction coefficient after optimization is lower than that before optimization. This indicates that the optimized microchannel structure (*A*=0.37 μm, *B*=10.96 μm, *C*=68.39°) achieves a more optimal pressure field distribution.

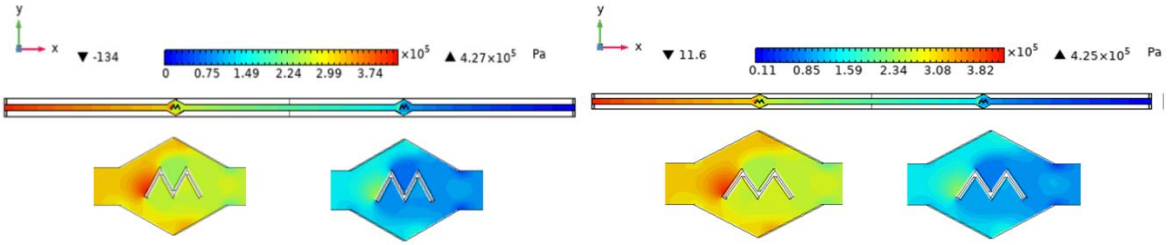

(a) (b)

Figure 6. Pressure diagrams before and after microchannel optimization (a) Pressure diagram before optimization (b) Pressure diagram after optimization

The temperature diagrams before and after the optimization of the microchannel are shown in Fig7. Compared to before the optimization, the temperature distribution is more uniform, and the highest temperature value has decreased. The Nusselt number is an important indicator reflecting the convective heat transfer capability in microchannels, the higher the convective heat transfer coefficient, the larger the Nusselt number, the opposite is smaller. According to the data in Tab7, the Nusselt number after optimization is higher than that before optimization. This indicates that the optimized microchannel structure (*A*=0.37 μm, *B*=10.96 μm, *C*=68.39°) achieves a better temperature field distribution.

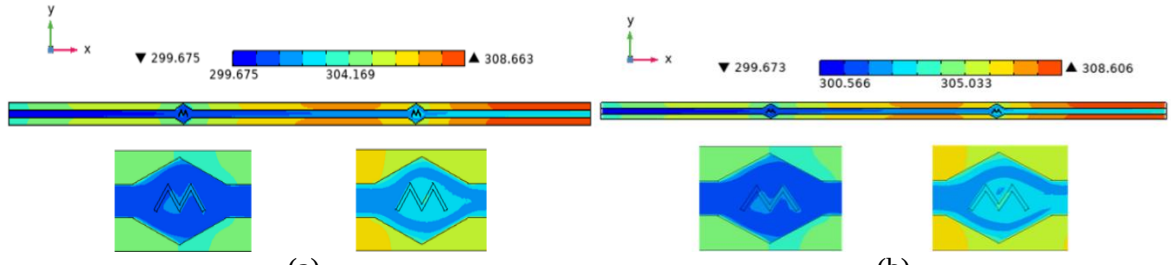

(a) (b)

Figure 7. Temperature diagrams before and after microchannel optimization (a) Temperature diagram before optimization (b) Temperature diagram after optimization

In previous work, we have completed the optimization design of the microchannel structure proposed by Alfellag et al[25]. The velocity distribution diagrams and temperature distribution diagrams of the newly proposed triangular cavity M-type pin microchannel structure in this paper, compared with

the original Alfellag microchannel structure[23] and the optimized Alfellag microchannel structure[25], are shown in Fig8. It can be clearly seen from the three velocity diagrams (a, b, and c) in Fig8 that at the cavity section where the microchannel height is 250 microns, the flow velocity at the cavity boundary of the triangular cavity M-type pin microchannel is higher than that of the trapezoidal cavities of both the original and optimized Alfellag structures. Specifically, its maximum velocity is 0.8 m/s higher than that of the original Alfellag microchannel structure and 0.2 m/s higher than that of the optimized Alfellag microchannel structure. This is because when the fluid enters the cavity and is separated to both sides by the pins, the M-type pins exert a stronger squeezing effect on the fluid than the elliptical pins. This stronger squeezing can more effectively enhance the disturbance of the fluid in the cavity, thereby significantly increasing the velocity at the cavity boundary. In addition, multiple eddies are formed at the corners of the M-type pins. These eddies disturb the fluid boundary layer and further promote the mixing of hot and cold fluids, which also lays a foundation for a more uniform temperature distribution in the microchannel.

Based on the above flow characteristics of the fluid in the microchannel and combined with the three temperature diagrams (d, e, and f) in Fig8, it can be found that at at the cavity section where the microchannel height is 250 microns, compared with the trapezoidal cavities of the original and optimized Alfellag structures, the triangular cavity M-type pin microchannel has a smaller maximum surface temperature and a more uniform temperature distribution. Therefore, compared with the Alfellag structure and the optimized Alfellag microchannel heat sink structure, the triangular cavity M-type pin microchannel heat sink shows better advantages in heat dissipation performance. It can remove heat more efficiently and provide a better solution for microchannel cooling systems.

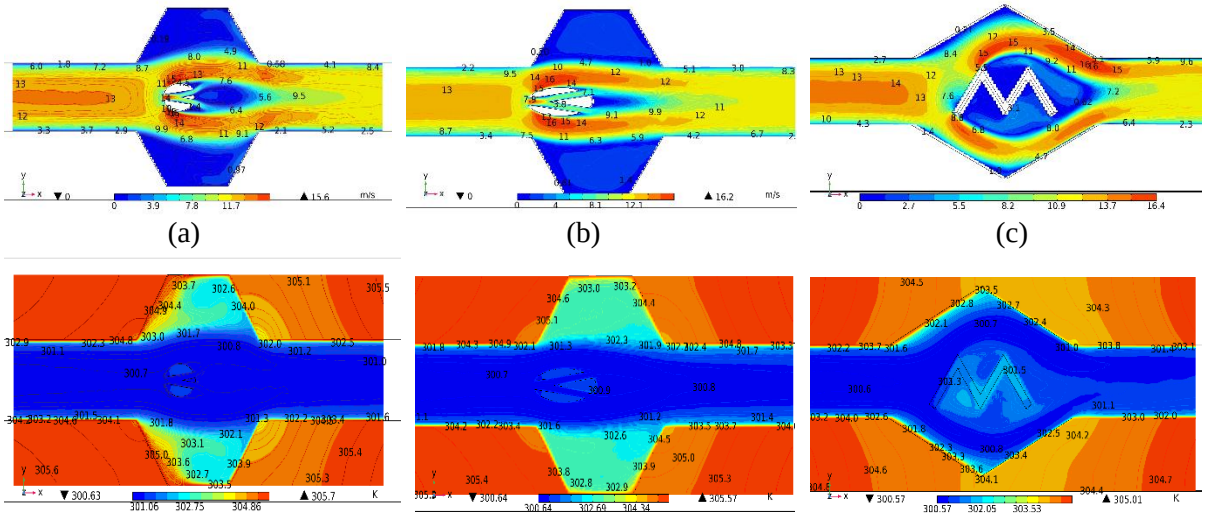

Figure 8. Velocity and temperature diagrams of different microchannel structures (a)-(c) Velocity for original Alfellag structure, optimized Alfellag structure and structure proposed in this paper (d)-(f)Temperature for the same setups

5. Conclusions

To address the heat dissipation issue of high thermal flux density in microelectronic devices, this paper proposes a novel triangular cavity M-type pin microchannel structure. In this paper, the polynomial functions of the distance between the center of the cavity type and the center of the pin, the pin width, the pin angle and the microchannel enhanced heat transfer factor are fitted by the response surface method. Then, the geometric parameters of the optimal microchannel structure were obtained by combining with genetic algorithm, so as to maximize the enhanced heat transfer factor. The paper draws the following conclusions.

(1) The closer the distance between the cavity center and the pin center, the stronger the turbulence of the fluid in the microchannel at the M-type pin, and the M pin promotes the full mixing of hot and cold fluids, thereby significantly improving the heat transfer efficiency of the microchannel.

(2) As the pin width decreases, the M-type pin will have a correspondingly larger contact area with the water flow, and the flow strength will also increase, which will significantly improve the heat transfer efficiency of the microchannel. However, this design change also leads to a rapid increase in the overall pressure drop of the microchannel, which weakens the enhanced heat transfer performance of the microchannel to a certain extent.

(3) When the angle of the M pin increases, the turbulence at the pin is weakened, which reduces the mixing efficiency of the hot and cold fluids, resulting in a decrease in the heat transfer performance of the microchannel. However, the increased angle of the M pin helps to reduce the overall pressure drop of the microchannel, which is beneficial for the energy consumption and operational efficiency of the system.

(4) The optimal microchannel structure (A=0.37 μm, B=10.96 μm, C=68.39°) and the optimal value of the enhanced heat transfer factor were 1.84, which could achieve the optimal distribution of pressure and temperature fields. This optimization method significantly improves the comprehensive heat transfer performance of microchannel, and provides an important engineering reference for the optimal design of structural parameters of microchannel heat sinks.

6. References

[1] Ohadi, M., et al., A comparison analysis of air, liquid, and two-phase cooling of data centers, 2012 28th Annual IEEE Semiconductor Thermal Measurement and Management Symposium (SEMI-THERM), San Jose, CA, USA, 2012, Vol. 1, pp. 58-63.

[2] Tuckerman, D. B., Pease, R. F. W., High-performance heat sinking for VLSI, IEEE Electron Device Letters, 2 (1981), 5, pp.126-129.

[3] Vinoth, R., Senthil, K. D., Numerical study of inlet cross-section effect on oblique finned micro channel heat sink, Thermal Science, 22 (2018), 6, pp. 2747-2757

[4] Acharya, S., Thermo-fluidic analysis of microchannel heat sink with inline/staggered square/elliptical fins, International Communications in Heat and Mass Transfer, 147 (2023), pp.106961.

[5] Wen, H. ,et al., Heat transfer performance study of microchannel heat sink with composite secondary channels, International Communications in Heat and Mass Transfer, 143 (2023), pp.106718.
[6] Wu, H. et al., Numerical study on flow and heat transfer characteristics in manifold microchannel heat sinks with rectangular restrictors, International Journal of Heat and Fluid Flow, 114 (2025), pp.109823.
[7] Hu, C., et al., Optimizing the performance of microchannel heat sinks: Effects of trapezoidal cover plate on flow boiling heat transfer and stability, International Journal of Heat and Mass Transfer, 244 (2025), pp.126942.
[8] Hajialibabaei, et al., Experimental and numerical study on heat transfer performance of wavy channel heat sink with varying channel heights, International Communications in Heat and Mass Transfer, 148(2023), pp.107044.
[9] Shi, et al., Optimal design on irregular polygon topology for the manifold micro-pin-fin heat sink, International Communications in Heat and Mass Transfer, 141(2023), pp.106574.
[10] Kamsuwan, C., et al., Enhancing performance of oblique double layer plate microchannel heat exchanger by computational fluid dynamics: Design and performance optimization, International Journal of Heat and Mass Transfer, 242 (2025), pp.126865.
[11] Fathi, et al., Bifurcated divergent microchannel heat sinks for enhanced micro-electronic cooling, International Communications in Heat and Mass Transfer, 146 (2023), pp.106868.
[12] Kang, et al., Investigation of heat transfer performance of the manifold microchannel heat sink with different interface configurations, International Communications in Heat and Mass Transfer, 159 (2024), pp.107807.
[13] Amit, et al., Heat transfer characteristics of pulsatile flow through microchannel with heat-spots: Mimicking heat generation in the blood vessels, International Communications in Heat and Mass Transfer, 159(2024), pp.108296.
[14] Liu, et al., Heat transfer enhancement of latent functional thermal fluid in microchannel with pin fins, International Journal of Heat and Mass Transfer, 244(2025), pp.126921.
[15] Zhou, Y., et al., Numerical analysis of enhanced heat transfer and nanofluid flow mechanisms in fan groove and pyramid truss microchannels, International Journal of Heat and Fluid Flow, 109 (2024), pp.109559.
[16] Bouaraour, K., et al., Mixed convection analysis of nanofluid flow inside an indented micro-channel, Thermal Science, 28 (2024), 5B, pp. 4321–4331.
[17] Jiang, M., et al., Optimization of open micro-channel heat sink with pin fins by multi-objective genetic algorithm, Thermal Science, 26 (2022), 4B, pp. 3653–3665.
[18] Rabiee, et al., Multi-objective optimization of rectangular microchannel heat sink based on entropy generation and hydro-thermal performance using NSGA-II algorithm, International Communications in Heat and Mass Transfer, 149 (2023), pp.107140.
[19] Wu, B., et al., Constructal design of a hybrid heat sink with rectangular microchannel and porous fin in a 3D electronic device with artificial neural-network, NSGA-II and different decision-making methods, International Communications in Heat and Mass Transfer, 158 (2024), pp.107954.
[20] Zhang, et al., Multi objective optimization of manifold microchannel heat sink with staggered microchannels, International Communications in Heat and Mass Transfer, 159(2024), pp.108106.
[21] Cheng, et al., Three-dimensional numerical investigation on flow and heat transfer characteristics and multi-objective optimization of interconnected microchannels, International Communications in Heat and Mass Transfer, 159(2024), pp.108102.
[22] Wang, Y., Qi, C. Multi-objective optimization on thermal–hydraulic performance of symmetrical hierarchical microchannel heat sinks, Applied Thermal Engineering, 271 (2025), pp.126309.

[23] Alfellag, M. A., et al., Optimal hydrothermal design of micro-channel heat sink using trapezoidal cavities and solid/slotted oval pins, Applied Thermal Engineering, 158 (2019), pp.113765.
[24] Webb, R. L. Performance evaluation criteria for use of enhanced heat transfer surfaces in heat exchanger design, International Journal of Heat and Mass Transfer, 24(1981),4, pp.715-726.
[25] Jiang, M., et al., Optimization of micro-channel heat sink based on genetic algorithm and back propagation neural network, Thermal Science, 27 (2023), 1A, pp. 179 – 193.

Paper submitted: 17.05.2025
Paper revised: 29.07.2025
Paper accepted: 05.08.2025